

Beam–gas recoil spectra of highly ionised neon

C.T. Chantler

Quantum Metrology Division, National Institute of Standards and Technology, Gaithersburg, MD 20899, USA

J.M. Laming¹

Naval Research Laboratory, Code 4174L, E.O. Hulburt Center for Space Research, Washington DC 20375-5000, USA

J.D. Silver

Clarendon Laboratory, Physics Department, University of Oxford, Parks Rd, Oxford, OX1 3PU, UK

Received 22 April 1992 and in revised form 4 September 1992

Observations of neon gas recoil spectra from bromine ion bombardment at 81–83 MeV energies are reported. Hydrogenic and helium-like ions were observed with a resolving power of 225. This is improved over previous work with the exception of narrow-range high-precision results of Laming et al. (Phys. Lett. A123 (1987) 395; Phys. Lett. A126 (1988) 253). Current data complementary to these narrow-range results provide wavelengths which show improved agreement with theory compared to earlier work.

1. Introduction

The main advantage of recoil ions as a spectroscopic source is that ions of interest have much lower velocities compared to other sources. Doppler shifts and broadening of spectral lines are therefore reduced. They can thus provide good resolution data on transitions of interest in astrophysical or tokamak plasmas, and hence yield information on the physics of these latter systems.

Often this work is limited to gas targets [1,2], but appropriate methods allow application of the same technique to solid [3,4]. Nonetheless, monatomic noble gases remain the forte of such investigations, which are sufficiently precise to provide significant measurements of QED effects in argon [5]. With argon however, severe satellite problems limit the attainable precision of measurement. For neon this is still significant but less severe, and the dominant difficulty lies with problems of instrumental resolution at these soft X-ray energies.

This work and simultaneous efforts [1,2] have addressed this problem directly and in a complementary way. Wavelengths and relative intensities for hydro-

genic through beryllium-like transitions between 11.2 and 14.1 Å are reported here.

2. Experimental

The source of ions for the experiment was the Oxford University Folded Tandem accelerator. A 1.5 mm diameter beam of $^{79}\text{Br}^{8+}$ at energies of 81–83 MeV was used. Typically 200–400 nA of current were produced. The gas target was differentially pumped and held at a stable pressure of approximately 53 Pa (0.4 Torr) of Ne, using diffusion pumps upstream and downstream of 5 mm diameter, 40 mm long apertures, while the adjacent beam-line remained at moderate (1.3×10^{-3} Pa, 10^{-5} Torr) vacuum. Collisions with gas atoms prior to the 60 mm-long detection region ensured that equilibrium charge-state distribution from +14 to +16 was achieved for incident 83 MeV bromine +8 beams. X-ray de-excitation from recoil ions was observed by a $R = 127$ mm (5 in.) Johannson Rowland circle scanning spectrometer, mounted normal to the beam and 37.5° to the vertical [6]. The 20 mm diameter entrance was covered by a 1.5 μm polypropylene window to maintain the spectrometer at 1.3×10^{-4} Pa (10^{-6} Torr) with pumping from a diffusion pump mounted below. A second 1 μm aluminium-coated Mylar window sealed the flow proportional counter

¹ Also: SFA, Inc., Landover, MD 20785, USA.

Correspondence to: Chris Chantler, Quantum Metrology Division, NIST, Bldg. 221, Rm. A141, Gaithersburg, MD 20899, USA.

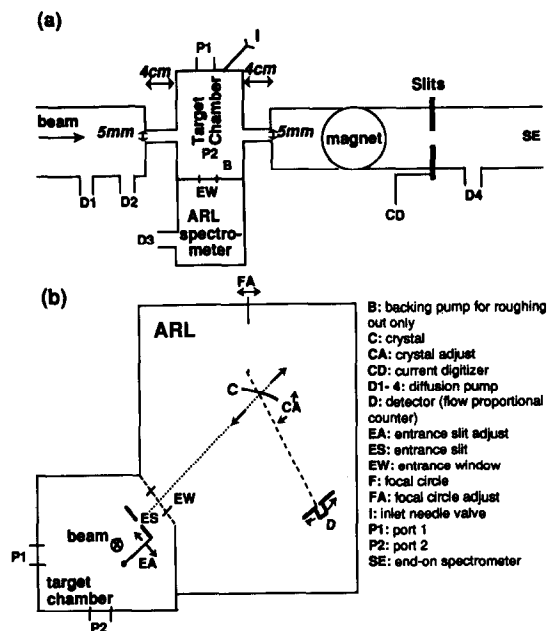


Fig. 1. Schematic of beam line and target chamber viewed (a) from above and (b) in cross-section of the target chamber and spectrometer. The solid target holder is inserted in port 2; a Si(Li) detector was used in port 1 to confirm identity of transitions. Resolution of the latter was inadequate for other purposes.

(P10 mixture, 90% Ar, 10% CH₄), and remotely-adjustable entrance and detector slits served to collimate the source. The entrance slit width was adjustable from $\delta x = 0.25$ mm to $\delta x = 2$ mm, with slit height 20 mm, mounted near the Rowland circle, and the detector slit was micrometer-driven and adjustable from 0.01 to 2 mm. Normalisation of integrated charge was achieved using a Faraday cup mounted downstream. Fig. 1 gives a schematic of the beam line and target chamber.

Germanium 220 and RAP (rubidium acid phthalate) 001 crystals were used in this experiment, each 12.7 mm \times 44.5 mm and ground to the $R = 127$ mm Rowland circle radius. Germanium crystals were used with a ⁵⁵Fe source to detect 5.89 keV Mn K α radiation and provide a test of the geometry and detection system. An Al K α X-ray source also provided confirmation of the geometry at 1.49 keV, 8.340 Å, with the RAP crystal.

Two crystals were mounted in the spectrometer on a mechanical assembly which permitted convenient external switching from one to the other as required. Spectra were scanned using a data collection programme UVRUN on the Oxford Nuclear Physics cluster. The stepping process was implemented by simultaneously increasing the distance from the entrance window to the crystal, tilting the axis of the crystal so that

the surface is tangential to the Rowland circle, and rotating the detector and detector slit to receive the appropriate wavelength. The resolving power $R = \lambda/\delta\lambda = x/\delta x$ varies with angle as a function of the distance x between these slits, which varies in turn from 200 to 770 mm from low to high wavelength limits [7].

For neon excitation, the RAP crystal was used, whose (001) reflection has a lattice spacing of $2d = 26.134$ Å [8], and permits observation of spectra from Mg K α to F K α in first order. This corresponds to a range of Bragg angles from 15° to 71°. Rocking curves for flat perfect crystals may be estimated from Burek [8], yielding resolving powers of $R = \lambda/\delta\lambda_{\text{FWHM}} \approx 1000$ for RAP. In our case, the performance was limited by crystal preparation and slit widths (as noted above), giving values of $x/\delta x$ of around 300.

3. Analysis and results

The most complete spectrum (labelled NECC) used an entrance slit width of 0.6 mm and detector slit width 0.16 mm, with a beam current of 400 nA 81 MeV Br⁹⁺ (1 MeV/amu). Fig. 2 indicates the line positions and spectral quality. This yielded a resolving power $R = 205$, which was less than two other runs, but with a higher

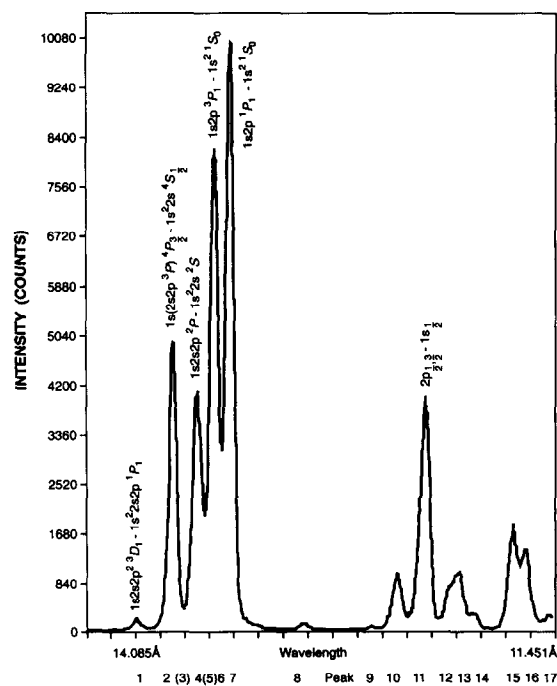


Fig. 2. Neon recoil spectrum NECC with peak and dominant satellite identification (q.v. table 1).

signal to noise ratio $s/n > 250$. Integrated counts for the dominant $1s2p^1P_1-1s^2\ 1S_0$ helium-like transition were 107 000 in the 10 channels corresponding to the FWHM after collection of 12 μC per channel, thereby providing good statistics. The highest resolution scan (NECE) used a detector slit of 0.11 mm under similar conditions, and yielded a resolving power $R = 225$ and signal to noise ratio $s/n \approx 120$. Hence, integrated counts for the same transition were 90 000 after accumulation of 20 μC (analysed) per channel, each channel step being 0.75 of the width of those used for NECC (circa 4.5 mÅ, versus 6.0 mÅ). This allows estimates of absolute cross-sections, but with large inherent uncertainty regarding charge state, diffraction and window efficiency and geometry. Normalised intensities are therefore reported in the following.

Spectra were calibrated following the linear relation of the spectrometer's stepping geometry $\lambda = Ax + B \text{ \AA}$, where x is the dial reading. The constants were over-determined using the four strongest and best-resolved spectral lines to give $\lambda = [x + 241.8 \pm 0.3]/[158.98 \pm 0.02] \text{ \AA}$. Results for NECE use three calibration lines only (not Lyman α), so have larger uncertainty away from the helium-like resonance lines. Calibration of NECC with the three lines alone yields a measurement of the mean Lyman α wavelength of 12.137 \AA , as opposed to 12.134 \AA in table 1, which confirms the overall linearity and precision. Agreement with earlier scans of lower resolution and s/n ratio was obtained, demonstrating the consistency of the results. Further details are given in ref. [6]. Table 1 compares these results to theory and alternate experimental values.

Table 1
Fitted wavelengths, identification and comparison: Neon recoil target spectra NECC, NECE

| Peak | $\lambda (\text{\AA})^a$ | $I (\%)^b$ | Identification ^c | Theory ^d | Experimental ^d |
|-------------|--------------------------|------------|--------------------------------------|---------------------|---------------------------|
| 1 | 14.085(9)(5) | 1.4 | NeVII $1s2s2p^{23}D_1-1s^22s2p^1P_1$ | 14.080v | |
| 2 α | 13.836(4) | 47.5 | NeVIII $1s(2s2p^3P)^4P-1s^22s^4S$ | 13.835w | 13.85b |
| | | | NeVIII $1s2p^{24}P-1s^22s^4S$ | 13.84b | |
| 3 | {13.731(5)} | 6.7 | NeVIII $1s2p^{22}D-1s^22p^2P$ | 13.71w | |
| | | | NeVIII $1s(2s2p^3P)^2P-1s^22s^2S$ | 13.71w | |
| | | | NeVIII $1s2p^{22}P-1s^22p^2P$ | 13.675k,w | 13.68b |
| 4 | 13.667 β (9)(4) | 50.9 | NeVIII $1s2s2p^2P-1s^22s^2S$ | 13.652,4k,w | |
| 5 | {13.600(5)} | 17.8 | NeVIII $(1s2p^3P)3d^4F-1s^23d^2D$ | 13.596w | 13.599(2) |
| | | | NeVIII $(1s2p^3P)3p^4P-1s^23p^2P$ | 13.589w | 13.591(1) |
| | | | NeVIII $(1s2p^3P)3d^2D-1s^23d^2D$ | 13.580w | 13.570(2) |
| | | | NeVIII $1s(2s2p^1P)-1s^22s^2S$ | 13.564w | 13.560(2) |
| 6 α | 13.552(47)(4) | 82.2 | NeIX $1s2p^3P_1-1s^{21}S_0$ | 14.5531d,490k | 13.57b |
| 7 α | 13.448(51)(4) | 100 | NeIX $1s2p^1P_1-1s^{21}S_0$ | 13.4473d | 13.46b |
| 8 | 12.949(7)(4) | 1.15 | NeVII $2s2p^3-1s2s2p^2$ | | 12.66r |
| 9 | 12.492(88)(4) | 0.61 | NeVIII $2s2p^{24}P-1s2s2p^4P$ | 12.480r | 12.51b,12.487r |
| 10 β | 12.316(20)(5) | 12.5 | NeIX $2p^{21}D_2-1s2p^1P_1$ | 12.355k | 12.34b |
| 10 β | | | NeIX $2s2p^3P_{2,1}-1s2s^3S_1$ | 12.303k,5,8w | |
| | | | NeIX $2s2p^1P_1-1s2s^1S_0$ | 12.260w | 12.14b |
| | | | NeIX $2p^{21}S_0-1s2p^1P_1$ | 12.172w | |
| 11 α | 12.134(4) | 47.4 | NeX $2p_{1/2}-1s_{1/2}$ | 12.1375j,60k,w | 12.14m |
| 11 α | | | NeX $2p_{3/2}-1s_{1/2}$ | 12.1321j,00k,w | |
| | | | NeIX $2p^{21}S_0-1s2p^3P_1$ | 12.087w | |
| 12 | 11.974(10) | 6.7 | NeVIII $1s2p3p-1s^22p$ | 11.96w | 12.00b,m |
| | | | NeVIII $(1s2s^3S)3p^4P-1s^22s^2S$ | 11.96c | 11.93b |
| 13 | 11.904(5) | 11.9 | NeVIII $(1s2s^3S)3p^2P-1s^22s^2S$ | 11.905k | 11.88m,93b |
| 14 | 11.798(5) | 3.2 | NeVIII $(1s2s^1S)3p^2P-1s^22s^2S$ | 11.83c | 11.80b |
| | | | NeIX $1s3p^3P_1-1s^{21}S_0$ | 11.58b | 11.56b,m |
| 15 | 11.536(6) | 18.3 | NeIX $1s3p^1P_1-1s^{21}S_0$ | 11.544k | 11.56b,m |
| 16 | 11.451(6) | 14.9 | NeVIII $(1s2l)4p[1s2p4p-1s^22p]$ | 11.476b | 11.47,8b |
| | | | NeVIII $1s2s3p^2P-1s^22s$ | 11.3w | |
| 17 | 11.293(10) | 4.0 | NeVIII $(1s2l)5p[1s2s5p-1s^22s]$ | 11.291b | 11.30,26b |
| | | | NeVIII $(1s2l)6p[1s2s6p-1s^22s]$ | 11.10b | 11.15b,m |

^a the fitting error in the last significant digits is quoted; curly brackets {} refer to (last digits of) highest resolution scan NECE.

^b integrated intensity is given relative to $1s^2-1s2p^1P_1$.

^c NeVII refers to Ne^{6+} transitions; $1s2s2p^2$ etc. gives the term values.

^d References are denoted by the letter: l = ref. [1]; b = refs. [12,13]; m = ref. [14]; j = ref. [16]; w = ref. [17]; k = ref. [18]; d = ref. [19]; c = ref. [20]; r = ref. [21]; v = ref. [22]. Quoted theoretical uncertainty lies at or below last digit.

α : used as reference line; β : double or unresolved peak.

4. Comparison to other experimental values, and to theory

In addition to this fitting error, there are uncertainties regarding satellite contamination discussed in ref. [1], a simultaneous high-resolution axial observation. There a FWHM of 0.018 Å was obtained for the $1s2p^3P_1-1s^2S_0$ transition, or a resolving power of 750. The study revealed satellite contributions to the 3P_1 and 1P_1 strongest components of total relative intensity 20% and 30% at 0.011 Å on the high wavelength side (from lithium-like transitions). A shift of the current spectra by less than 0.002–0.003 Å would therefore be expected. This is less than the fitting error. It could be similar for Lyman α , and considerably less for the lithium-like NeVIII $1s(2s2p^3P)^4P_{3/2}-1s^22s^4S_{1/2}$ transition (due to the selective charge-state population). Uncertainty in the theory and calculation of calibration wavelengths contributes at the 0.001–0.01 Å level; this is supported by the agreement obtained to 0.002–0.009 Å for relative satellite locations in the above study.

Ref. [2] reports a high-resolution beam-foil measurement of hydrogenic neon. This resolving power $R \approx 4800$ partially separates the Lyman α doublet and shows no major structure, but was produced in a fast-beam rather than a recoil source, so does not demonstrate purity of the recoil source for these transitions. Doppler uncertainty lies at the 10% level, preventing accurate QED measurement of the transitions, and limiting relative measurements (with fitting and energy loss uncertainty).

Quoted results of ref. [10,11] provided a resolving power of 140 under similar conditions, but no tabulation of results was given. Beyer, Mann, and Folkmann made a series of detailed studies with resolving power of approximately 200 and found cleanest excitation for low-velocity highly charge ions (1.4 MeV/amu Kr^{18+} , Xe^{24+} , Pb^{36+}) [12–15], similar to conditions used here. Higher charge states are observed at lower pressures, where the mean time between collisions is longer. Agreement with their derived wavelengths is good, but the current results give significantly close agreement with theory, and suggest overall improvement by significant factors for peaks 10–17, in particular.

The nature and precision of theoretical calculations differs greatly for different wavelengths listed in table 1. Hydrogenic Lyman α transitions (line 11) are extremely precise, as partially indicated by the variation between the computed values. The first value listed [16] is accurate to all significant figures, while the latter value [17,18] is discrepant by the amount shown. Equally, QED, relativistic and electron correlation effects are included to high order and precision for helium-like resonance transitions computed by ref. [19] (lines 6 and 7), as opposed to values indicated in table 1 with letters (b, w, k, c, r, v) for refs. [12,13,17,18,20–

22]. This partially justifies the use of reference lines given, and indicates that the major results of this study (apart from intensity ratios) relate to measurements of non-resonant helium-like transitions and to lithium-like transitions. For these the theoretical calculations have not advanced to the same level of precision, and omit electron correlation, QED and relativistic contributions to transition energies of varying size and significance. The size and significance involved is then indicated in the table to be, for example, 0.021(5) Å for the discrepancy of ref. [17] for line 3, 0.017(4) Å for ref. [18] and line 4, 0.012(4) Å for ref. [21] and line 9 and 0.032(5) Å for ref. [20] and line 14. Most other lines appear to agree with theoretical computation to within two standard deviations of experiment.

5. Conclusions

The present work indicates transitions for which improved calculation of correlation or other effects appear to be necessary. Many of these effects are large for particular lines and very small for others, and closer investigation of the cause of individual discrepancies could hopefully lead to improved calculations and overall tabulations, and to a better understanding of the theory. Until then, the results provide measurements which can be used in tokamak, astrophysical and other plasma studies for diagnostic or spectroscopic investigations.

1s Lamb shift measurements have not been made in neon (by recoil or other methods), since standard (RAP) crystal resolutions are inadequate to separate the two Lyman α components. A resolution of 2200 is required to separate them by $\delta\lambda_{FWHM}$, and QED effects are 33% of their separation. Optimum crystals such as KAP in second order ($\lambda/\Delta\lambda = 4000$) only approach the required resolution. The prospect for this technique to provide sensitive measurement of QED processes in neon is, therefore, dim. However, the range of Z between oxygen and argon is accessible by this technique for medium to high resolution spectroscopy. QED effects may well become viable with the advent of suitable solid target geometries, or of vapour phase investigations of Na, Mg, Al, etc. There crystal resolution is fully adequate to the problem of QED measurements and satellite difficulties may remain negligible. The information gained from these studies will be of use in future recoil experiments and in studies of these ions in other plasmas.

Data are consistent with a beam-target interaction stripping most electrons from the gas target leaving 2p, 1s2l and 1s2l2l' states predominantly. Slow recoil ions in 1s2l states capture electrons from neutral gas atoms into 3p or 4p states before cascading and decaying. Capture selectivity follows from matching the (mod-

ified) ionisation potential of the neutral gas to the electron binding energy in the highly-ionised atom for principal quantum number n [12–14]. This model is well-supported and applicable to monatomic gas recoils. Recoil energies are in the range 10–70 eV (from Auger electron and other studies). The non-statistical nature of the interaction has been established. Further developments could pursue other energy regimes, targets and spectral regions following the recoil-ion basis indicated here.

The improvement in resolving power and calibration represented herein has led to confirmation of the recoil-ion technique and a significant improvement in experimental precision and accuracy.

Acknowledgements

The authors acknowledge the support and expertise of the Oxford Folded Tandem accelerator staff. One author (C.C.) would like to thank Shell Australia, St. Anne's College, Oxford, the ESU for a Lindemann Fellowship, and NIST.

References

- [1] J.M. Laming, Ph.D. thesis, University of Oxford (1988); J.M. Laming and J.D. Silver, *Phys. Lett.* A123 (1987) 395.
- [2] J.M. Laming, J.D. Silver, R. Barnsley, J. Dunn, K.D. Evans and N.J. Peacock, *Phys. Lett.* A126 (1988) 253; J. Dunn, Ph.D. thesis, University of Leicester (1990).
- [3] C.T. Chantler and J.D. Silver, *Nucl. Instr. and Meth.* B31 (1988) 59.
- [4] C.T. Chantler, Ph.D. Thesis, University of Oxford (1990).
- [5] H.F. Beyer, R.D. Deslattes, F. Folkmann and R.E. LaVilla, *J. Phys.* B18 (1985) 207.
- [6] The spectrometer was obtained from Applied Research Laboratories, California. This identification does not imply endorsement nor should it be taken to suggest that the identified items are necessarily best suited for the applications in which they are used.
- [7] C.T. Chantler, First year D. Phil. report, University of Oxford (1986) unpublished.
- [8] R.A. Smith, *Acta Crystallogr.* B31 (1975) 2347.
- [9] A. Burek, *Space Science Instr.* 2 (1976) 53.
- [10] H.A. Klein, S. Bashkin, B.P. Duval, F. Moscatelli, J.D. Silver, H.F. Beyer and F. Folkmann, *J. Phys.* B15 (1982) 4507.
- [11] H.A. Klein, Ph.D. thesis, University of Oxford (1983).
- [12] H.F. Beyer, J.-H. Schartner, F. Folkmann and P. Mokler, *J. Phys.* B11 (1978) L363.
- [13] H.F. Beyer, K.-H. Schartner and F. Folkmann, *J. Phys.* B13 (1980) 2459.
- [14] R. Mann, F. Folkmann and H.F. Beyer, *J. Phys.* B14 (1981) 1161.
- [15] F. Folkmann, R. Mann and H.F. Beyer, *Physica Scripta* T3 (1983) 88.
- [16] W.R. Johnson and G. Soff, *At. Data Nucl. Data Tables* 33 (1985) 405.
- [17] L.A. Vainshtein, U.I. Safranova, *At. Data Nucl. Data Tables* 25 (1980) 311.
- [18] R.L. Kelly and L.J. Palumbo, *Atomic and ionic emission lines below 2000 Å*, NRL Report 7599 (1973).
- [19] G.W.F. Drake, *Can. J. Phys.* 66 (1988) 586.
- [20] M.H. Chen, *Phys. Rev.* A15 (1977) 2318.
- [21] R.L. Kauffmann, C.W. Woods, K.A. Jamison and P. Richard, *Phys. Rev.* A11 (1975) 872.
- [22] L.A. Vainshtein and U.I. Safranova, *At. Data Nucl. Data Tables* 21 (1978) 49.